IJIRSET
International Journal of Innovative Research in
SCIENCE | ENGINEERING | TECHNOLOGY

e-ISSN: 2319-8753 | p-ISSN: 2347-6710

INTERNATIONAL JOURNAL OF INNOVATIVE RESEARCH

IN SCIENCE | ENGINEERING | TECHNOLOGY

Volume 12, Issue 4, April 2023

ISSN INTERNATIONAL STANDARD SERIAL NUMBER INDIA

Impact Factor: 8.423

9940 572 462 | 6381 907 438 | ijirset@gmail.com | www.ijirset.com

International Journal of Innovative Research in Science, Engineering and Technology (IJIRSET)

|e-ISSN: 2319-8753, p-ISSN: 2347-6710| www.ijirset.com | Impact Factor: 8.423| A Monthly Peer Reviewed & Referred Journal |

|| Volume 12, Issue 4, April 2023 ||

| DOI:10.15680/IJIRSET.2023.1204220 |

Removal of Impulse Noise in Images using Adaptive Decision Tree Based Image Denoising

Mr Harikrishnan S[1] , Y. Yaswanth[2], K. Jagadeesh[3] , P. Thulasi Reddy[4] , R. Naveen Kumar Reddy[5], M. Jaswanth Reddy[6]

Head of Department, Sanskrithi School of Engineering, Puttaparthi, Andhra Pradesh, India[1]

Department of Electronics and Communication Engineering, Sanskrithi School of Engineering, Puttaparthi, Andhra Pradesh, India [2]

ABSTRACT: Impulse noise frequently taints images throughout the picture acquisition and transmission processes. For the removal of random-valued impulse noise, we suggest an effective denoising approach and its VLSI architecture in this study. It is suggested that a low-complexity VLSI design be used to realise the low cost objective. We use an edge- preserving filter to recover the intensity values of noisy pixels and a decision-tree-based impulse noise detector to find the noisy pixels. Additionally, the results of eliminating impulse noise are improved by the application of adaptive technology. Our extensive experimental findings show that the suggested strategy can outperform the earlier, lesser complexity methods in terms of quantitative evaluation and visual quality. Additionally, the performance may be equivalent to the more complicated system methods. Utilising TSMC 0.18 m technology, the VLSI architecture of our design produces a processing speed of roughly 200 MHz. This innovation can minimise memory storage by more than 99 percent compared to cutting-edge methods. Only two line memory buffers and low computational complexity are needed for the design. Its low hardware cost makes it appropriate for use in many real-time applications.

KEYWORDS: Saltand, Sludge, Quantifiable, Disparities

I. INTRODUCTION

IMAGE processing is extensively used in numerous fields, similar as medical imaging, surveying ways, printing chops, license plate recognition, face recognition, and so on. In general, images are frequently corrupted by impulse noise in the procedures of image accession and transmission. The noise may seriously affect the performance of image processing ways. Hence, an effective denoising fashion becomes a veritably important issue in image processing(1),(2). Accordingto the distribution of noisy pixel values, impulse noise can be classified into two orders fixed valued impulse noise and arbitrary- valued impulse noise. or its variations(9),(10). still, these approaches might blur the image since both noisy and noise-free pixels are modified. To avoid the damage on noise-free pixels, an effective switching strategy has been proposed in the literature(11),(12),(13). In general, the switching standard sludge consists of two way 1) impulse discovery and 2) noise filtering.

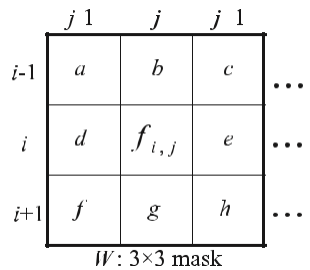

|e-ISSN: 2319-8753, p-ISSN: 2347-6710| www.ijirset.com | Impact Factor: 8.423| A Monthly Peer Reviewed & Referred Journal |

|| Volume 12, Issue 4, April 2023 ||

| DOI:10.15680/IJIRSET.2023.1204220 |

II. THE SUGGEST DTBDM

Based on the generalisations from the introduction above, we provide a new adaptive decision- tree- grounded denoising system (DTBDM) and its VLSI armature for removing arbitrary- valued impulsive noise. The results of the repaired pixels are provided back as input data in an adaptive manner to enhance the advantages of dumping impulsive noise. Since the proposed method just requires two line memory buffers and fundamental calculations, it has a low tackling cost. In our system, a 512 512 8-bit grayscale test image may be processed with just a two line buffer (512 2 8 bits). For an entire image, the most cutting-edge approaches require 512 512 8 bits of padding. In our design, we minimise 99.6% of the storage. Similar to how only fundamental mathematical operations like addition and subtraction are used by DTBDM. The performance may additionally resemble advanced complexity styles(14),(15), or(16). The seven-stage VLSI armature for the proposed design was enforced and synthesised independently using Verilog HDL and Synopsys Design Compiler. In our simulation, the circuit requires merely 21k TSMC 018 m gate counts to run at 200 MHz. Thisessay's remaining sections are organised as follows. The intended DTBDM is briefly described in The noise investigated in this work is arbitrary-valued impulse noise with an invariant

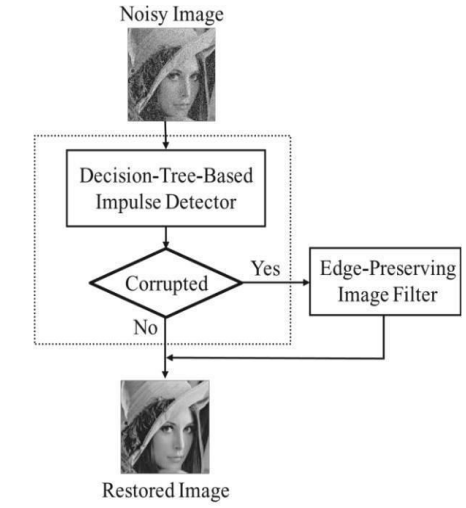

Fig. 2. The dataflow of DTBDM.

III. RELATED WORK

b, c, and dg 1 and WBottomHalf 14 fe, f, g, and hg 2 the outcomes of the calculation. The DTBDM consists of an edge-conserving image sludge and a decision-tree-based grounded impulse sensor. whether or not the sensor detects pi The decision tree's association with pixels pi and j To establish whether pi; j is a noisy pixel, the sensor looks at surrounding pixels.If the outcome is favourable, edgepreserving image sludge based on direction-aware sludge is used to construct the restored value. The value won't alter in that instance. Figure 2 depicts the DTBDM's design concept. 2.1 Decision Tree-Based Impulse Detector

Correlations between pi;j and its neighbouring pixels are taken into account to decide whether pi;j is a noisy pixel [10],[11], [14], [16], [17], [23], [24], [25], [26], [27], [28], [29], [30]. We can just List these methods in the order listed below

to classify them: observing [16], [17], [26], [27], or assessing the [10], [11], [14], [16], [17], [23], [24], [25], the degree of similarity between the current pixel and its neighbours, [16], [28], [29], and [30]. The isolation module (IM), fringe module (FM), and similarity module (SM) are the three modules we create for our decision-tree-based impulse detector.A decision tree is created by concatenating these three modules' judgements. Utilised is a decision tree. It is possible to

|e-ISSN: 2319-8753, p-ISSN: 2320-6710| www.ijirset.com | Impact Factor: 8.118| A Monthly Peer Reviewed & Referred Journal |

|| Volume 12, Issue 4, April 2023 ||

| DOI:10.15680/IJIRSET.2023.1204001 |

assess the condition of pi;j using a binary tree and the multiple equations from various modules. The isolation module isfirst used to determine whether the pixel value is in a smooth zone.

IV. METHODOLOGY

Isolation Module

As shown in Figure 3, the pixel values in a smooth zone should be comparable or barely differ locally. variations in the values of A small number of pixels around it. The distribution of the values alters whether there are noisy values, edges,or blocks in this area, as seen in Fig. 4. As a result, we can tell if a pixel is an isolation point by looking at how smooth the pixels around it are. An example of a noisy image is shown in Fig. 5. There aren't many similarities between the apparently isolated location and the shaded noise-affected pixels. Its value is very different from the surrounding pixels. The maximum and lowest luminance values in WTopHalf are identified as TopHalf_max and TopHalf_min, respectively, and their difference, TopHalf_diff, is then calculated using the above-mentioned principles. The same concept is used toobtain BottomHalf_diff for WBottomHalf. To assess whether the surrounding area is smooth, the two difference values are contrasted with a threshold T h IMa.

Fringe Module

If pi;j differs significantly from its neighbours, it may be a noisy pixel (described in Section 2.1.1 IM) or simply be located on an edge, as depicted in Fig. 6. It is challenging to determine if a pixel is noisy or located on an edge. We establish four directions, from E1 to E4, as shown in Fig. 7, to deal with this situation. Take, for instance, direction E1. We can identify whether or not there is an edge by computing the absolute difference between fi;j and the other two pixelvalues along the same direction, respectively. The exact formulae are as follows.

Module for Similarity

Similarity is the final module. mask W's brightness values are situated in A quiet region can be nearby. The impulse typically lies close to one of the variational series' ends, but the median always lies in the middle. As a result, excessivelyhuge or tiny values indicate the potential for noisy signals. With this idea in mind, we order nine values ascendingly to get the fourth, fifth, and sixth values, which are quite near to the median in mask W. The symbols for the fourth, fifth, and sixth values are 4thinWi;j, MedianInWi;j, and 6thinWi;j, respectively. Maxi;j and Mini;j are defined as

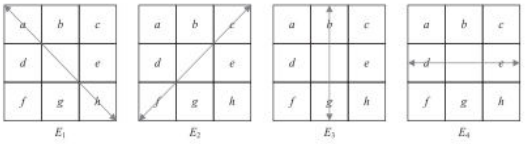

Fig. 7. Four directions in DTBDM.

$$\begin{aligned} Max_{i,j} &= 6_{th}inW_{i,j} + Th\_SM_a, \\ Min_{i,j} &= 4_{th}inW_{i,j} - Th\_SM_a. \end{aligned} \tag{14}$$

$Max_{i,j}$ and $Min_{i,j}$ are used to determine the status of pixel $p_{i,j}$. However, in order to make the decision more precisely, we do some modifications as

$$N_{\max} = \begin{cases} Max_{i,j}, & \text{if } (Max_{i,j} \le MedianInW_{i,j} \\ & \quad + Th\_SM_b) \\ MedianInW_{i,j} & \\ \quad + Th\_SM_b, & \text{otherwise.} \end{cases} \tag{15}$$

$$N_{\min} = \begin{cases} Min_{i,j}, & \text{if } (Min_{i,j} \ge MedianInW_{i,j} \\ & \quad - Th\_SM_b) \\ MedianInW_{i,j} & \\ \quad - Th\_SM_b, & \text{otherwise.} \end{cases} \tag{16}$$

Finally, if $f_{i,j}$ is not between N_{max} and N_{min}, we conclude that $p_{i,j}$ is a noise pixel. Edge-preserving image filter will be used to build the reconstructed value. Otherwise, the original value $f_{i,j}$ will be the output. The equation is as

$$Decision\ IV = \begin{cases} true, & \text{if } (f_{i,j} \ge N_{\max}) \text{ or } (f_{i,j} \le N_{\min}) \\ false, & \text{otherwise.} \end{cases} \tag{17}$$

|e-ISSN: 2319-8753, p-ISSN: 2347-6710| www.ijirset.com | Impact Factor: 8.423| A Monthly Peer Reviewed & Referred Journal |

|| Volume 12, Issue 4, April 2023 ||

| DOI:10.15680/IJIRSET.2023.1204220|

It goes without saying that the threshold has an impact on the suggested method's denoised image quality. A better detection result can be attained with a more suitable threshold. The analytical construction of an ideal threshold is challenging, though. Our approach is straightforward and suited for hardware implementation because the threshold values are fixed.

V. IMPLEMENTATION

DTBDM's cost of VLSI implementation is inexpensive due to its low computational complexity and need for only twoline buffers as opposed to full pictures. We use the pipelined architecture, which generates an output once every clock cycle, to improve timing performance. In our implementation, the 512 8-bit SRAMs that are utilised to hold the image luminance values are created using the 0:18 m TSMC/Artisan memory compiler [31]. We discover that the access timefor SRAM is around 5 ns based on simulation results acquired from Design Ware of SYNOPSYS [32]. So, for DTBDM, we employ the 7-stage pipelined architecture. Block diagram of the DTBDM VLSI design
In this work's hardware architecture, as illustrated in Fig. 12, the denoised value at coordinate i; j 1 is still in the pipeline and not yet available. Here, the 3 3 mask receives nine input pixels—six original points and three adaptive points—toreconstruct the pixel fi;j. Even though there are only three adaptive points, or less than half of the nine input points, the **Ping-Pong Buffer (Line Buffer)**
Three scanning lines are required because DTBDM uses a 3 3 mask. Three pixels from rows 1, 2, and 1 are required to complete the denoising procedure if pi;j are processed. Below, we writing back data concurrently) instead of a series of shifter registers. If the size of an image is Iw Ih, the size required for one line buffer is Iw 3 bytes in which 3 represents the number of pixels stored in the register bank.

Register Bank

The register bank, consisting of nine registers, is used to store the 3 3 pixel values of the current mask W. Fig. 12shows its architecture where each three registers are connected serially in a chain to provide three pixel values of a row in W, and the Reg4 keeps the luminance value ðfi;jÞ of the current pixel to be denoised. Obviously, the denoising process for $p_{i;j}$ doesn't start until f_{i}þ1;jþ1 enterersfrom the input device. The nine employ the ping- pong arranging principle. We implement three scanning lines with two line buffers using four crossover multiplexers(see Fig. 12). As illustrated in Fig. 12, the odd-line buffer and even-line buffer are intended to store the pixels at theodd and even rows, respectively. The line buffer is implemented with a dual-port SRAM (one

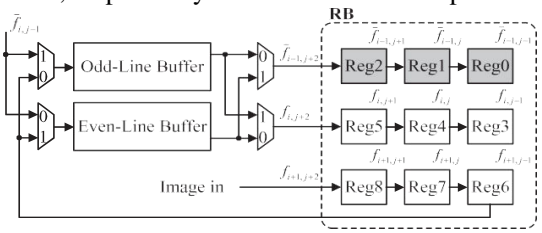

port for reading out
data and the other for writing data), which reduces the cost and power consumption.

Architecture of register bank in DTBDM.

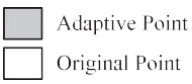

Two examples of the interconnections between two line buffersand RB.

|e-ISSN: 2319-8753, p-ISSN: 2347-6710| www.ijirset.com | Impact Factor: 8.423| A Monthly Peer Reviewed & Referred Journal |

|| Volume 12, Issue 4, April 2023 ||

| DOI:10.15680/IJIRSET.2023.1204220|

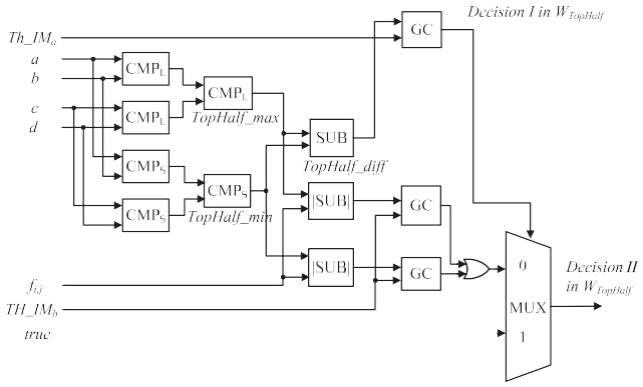

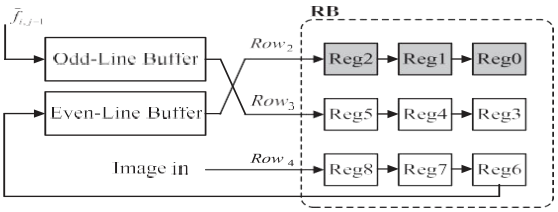

Decision-Tree-Based Impulse Detector

The decision-tree-based impulse detector is composed of three modules (isolation module, fringe module, and similaritymodule). Each of them is described in the following sections

Isolation Module

The comparator CMPL is used to output the larger value from the two input values while the comparator CMPS is used to output the smaller value from the two input values. The first two-level comparators are used to find TopHalf_max and TopHalf_min. The SUB unit is used to output the difference which is subtracted the lower input (TopHalf_min) from the upper one (TopHalf_max), and the jSUBj unit is used to output the absolute value of difference of two inputs. The GC is the greater comparator that will As seen samples of row 3 are inputted from the input device. Both the denoised outcomes produced by the edge-preserving filter and the preceding value in Reg6 are written back to the even- and odd-line buffers,respectively. Odd-Line Buffer is now completely filled with the whole samples of row3 following the completion of row2's denoising operation, while row2's denoised samples are all put in even-Line buffer. Row 3 is denoised by setting all selection signals to 1. As a result, as shown in Fig. 13b, the previous value in Reg6 and the denoised outcomes produced by the edge-preserving filter are written back to the relevant even-line buffer and odd-line buffer. Even-Line Buffer is now filled with data following the denoising of row 3 To output the absolute value of the difference between two inputs, use the jSUBj unit.

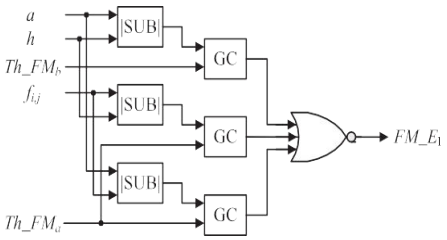

Fig. 15. Architecture of FM.

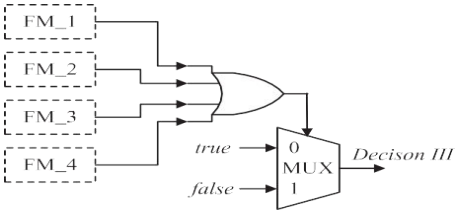

Fig. 16. Architecture of FM 1 module.

If the higher input value is bigger than the lower one, output logic 1. To provide the binary result for IM_TopHalf, the OR gate is used. Finally, pi;j might be a noisy pixel or be located on an edge if the outcome of Decision II is favourable. The outcome will be verified using the following module (FM).

Fringe Module

The architecture of FM is depicted in Fig. 15. As noted in Section 2.1.2, the FM is made up of four tiny modules, FM_1 through FM_4, each of which is utilised to establish its orientation. A thorough implementation of FM_1 is shown in Fig.

16. Since E1 (Fig. 7) represents the direction from a to h, it is necessary to refer to the relationship between a, h, and fi;j. that trio To calculate the absolute differences between them, utilise jSUBj units. The GC is discussed in the section above, and the FM E1 output is produced by the NOR gate. If the outcome is good, we assume that fi;j is on the brink of being noise-free and regard it as such.

|e-ISSN: 2319-8753, p-ISSN: 2347-6710| www.ijirset.com | Impact Factor: 8.423| A Monthly Peer Reviewed & Referred Journal |

|| Volume 12, Issue 4, April 2023 ||

| DOI:10.15680/IJIRSET.2023.1204220|

Module for Similarity

The finding is confirmed by SM if IM and FM are unable to establish whether fi;j is a part of a noisefree value or not. Our sorting architecture, which is depicted in Fig. 17, is intended to speed up the process of finding the fourth value in the mask W. Fig. 18 displays a detailed implementation of module M0. C01 is set to 1 if an is bigger than b; else, C01 is set to 0. The values from C01 through C08 are calculated using the eight GC units. Following comparison, each comparator's values are combined in a combined unit to provide a number between 0 and 8. The number represents the ranking of the values in mask W. The output of the M0 module is 0 if an is the smallest value in the mask W and 8 if an is the largest value. The structures of the remaining modules (M1 to M8) are largely identical to those of M0.

Fig. 18. Architecture of M0 module.

Edge-Preserving Image Filter, Version

The composition of the Edge-Preserving Image Filter consisting of the average generator (AG) and the minED generator. The architecture of the minED generator, which is utilised to identify the edge with the smallest difference, is shown in Fig. 20. In order to calculate eight directional differences, twelve jSUBj, four ADD, and four shifter units are used. The Min Tree unit is then used to determine which is the smallest. A number of comparators make up Min Tree. The average generator can then be used to determine the mean of the brightness values of the pixels that process the lowest directionaldifference, as shown in Fig. 21. As stated in Section 2, the final MUX will produce a b 2 c=4 if pi;j1; pi;j1; pi;j1; pi;j1; pi;j and pi;j1 are all thought to be noisy pixels. Without it, the The mean of the pixel values that Dmin processes will be output by MUX. Four pixel values are used to identify some directional disparities, hence its reconstructive values also require four pixel values.

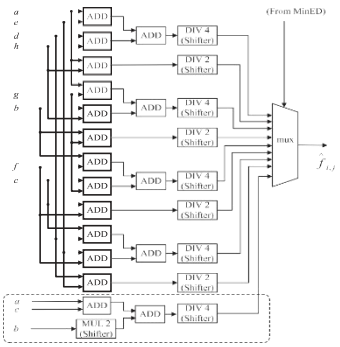

Fig. 21. Architecture of average generator.

|e-ISSN: 2319-8753, p-ISSN: 2347-6710| www.ijirset.com | Impact Factor: 8.423| A Monthly Peer Reviewed & Referred Journal |

|| Volume 12, Issue 4, April 2023 ||

| DOI:10.15680/IJIRSET.2023.1204220|

Experimental results

Comparative Results in PSNR (dB) of Images Corrupted by 15 Percent Impulses

	images / method	Comparative Results					
		Lena	Boat	Couple	Goldhill	Peppers	Airplane
L.C	Noisy	16.21	15.99	16.40	16.12	15.91	15.05
	median [8]	30.95	28.48	27.36	29.30	31.29	29.90
	ACWM [12]	32.81	30.50	29.45	31.26	32.30	31.07
	MSM (3:T) [13]	29.30	28.35	28.09	28.56	29.11	28.14
	MSM (5:T) [13]	28.66	27.82	27.70	28.02	28.41	27.43
	MSM (7:T) [13]	25.59	24.97	25.32	27.76	25.08	24.08
	RVNP [33]	31.14	28.92	27.84	29.94	31.42	30.12
	AMF [34]	31.70	29.30	28.49	30.22	31.49	30.23
	NAVF [35]	31.91	29.43	28.73	30.74	31.73	30.66
	LCNR [36]	34.07	30.95	29.39	31.81	32.96	32.38
	Proposed	34.43	31.38	30.10	32.21	33.70	32.73
H.C	ATMBM [14]	32.23	30.13	29.18	30.90	31.62	30.49
	DRID [15]	32.86	30.87	29.88	31.40	31.80	31.62
	RORD-WMF[16]	34.87	30.57	28.77	31.76	33.91	32.74

L.C = Lower Complexity;H.C = Higher Complexity

	Mask Size	Line Buffer	Iteration Times
Median filter [8]	3x3		
ACWM [12]	3x3	2	0
RVNP [33]	3x3	2 2	0 0
MSM (3:T) [13] MSM (5:T) [13]	5x5		
MSM (7:T) [13]	7x7	4	0
	3x3	6	0
AMF [34]	3x3	2	0
NAVF [35]	3x3	4 4	0 0
LCNR [36]	3x3	2	0
Proposed	3x3	2	0
ATMBM [14]	3x3	whole image	4
DRID [15]	5x5	whole image	4
DORD-WMF [16]	7x7	whole image	3

Table 6 displays the odds of impulse detection, including missed opportunities and false alarms. When a detector reports an impulse when there isn't, it is said to be a false alarm. We only mention comparisons between our approach and other greater complexity methods because the quantitative features of our method are significantly superior than those of other lower complexity methods. Iterative techniques used by ATMBM and DRID can lower the amount of misses, but they also result in more false alarms, as seen in Table 6. In comparison to those greater complexity systems,the overall numbers (misses + false alarms) in this work are significantly lower.

The images [15], [16], and [36] are superior to others, and we only use them for visual comparisons. There is noticeable noise in the photos that ACWM, ATMBM, and DRID have restored. Our method's reconstructed image can retain more information in the margins (see pepper stalk in Fig. 22). It is obvious that the suggested DTBDM results in attractive photographs. Verilog HDL was used to implement our design's VLSI architecture.

|e-ISSN: 2319-8753, p-ISSN: 2347-6710| www.ijirset.com | Impact Factor: 8.423| A Monthly Peer Reviewed & Referred Journal |

|| Volume 12, Issue 4, April 2023 ||

| DOI:10.15680/IJIRSET.2023.1204220|

VI. CONCLUSION

We have implemented an automatic text detection technique from an image for Inpainting. Our algorithm successfully detects the text region from the image which consists of mixed text-picture-graphic regions. We have applied our algorithm on many images and found that it successfully detect the text region.

REFERENCES

[1] M. Bertalmio, G. Sapiro, V. Caselles, and C. Ballester, "Image inpainting", in Proc. SIGGRAPH, pp. 417–424,2000.

[2] A. Criminisi, P. Perez, and K. Toyama, "Region filling and object removal by exemplar-based image inpainting.",IEEE Transactions on Image Processing, vol. 13, no.9, pp. 1200–1212, 2004.

[3] Marcelo Bertalmio, Luminita Vese, Guillermo Sapiro, Stanley Osher, "Simultaneous Structure and Texture ImageInpainting", IEEE Transactions On Image Processing, vol. 12, No. 8, 2003.

[4] Yassin M. Y. Hasan and Lina J. Karam, "Morphological Text Extraction from Images", IEEE Transactions On Image Processing, vol. 9, No. 11, 2000

[5] Eftychios A. Pnevmatikakis, Petros Maragos "An Inpainting System For Automatic Image Structure-TextureRestoration With Text Removal", IEEE trans. 978-1-4244-1764, 2008

[6] S.Bhuvaneswari, T.S.Subashini, "Automatic Detection and Inpainting of Text Images", International Journal ofComputer Applications (0975 – 8887) Volume 61– No.7, 2013

[7] Aria Pezeshk and Richard L. Tutwiler, "Automatic Feature Extraction and Text Recognition from Scanned Topographic Maps", IEEE Transactions on geosciences and remote sensing, VOL. 49, NO. 12, 2011

[8] Xiaoqing Liu and Jagath Samarabandu, "Multiscale Edge-Based Text Extraction From Complex Images", IEEETrans., 1424403677, 2006

[9] Nobuo Ezaki, Marius Bulacu Lambert , Schomaker , "Text Detection from Natural Scene Images: Towards a Systemfor Visually Impaired Persons" , Proc. of 17th Int. Conf. on Pattern Recognition (ICPR), IEEE Computer Society, pp. 683-686, vol. II, 2004

[10] Mr. Rajesh H. Davda1, Mr. Noor Mohammed, " Text Detection, Removal and Region Filling Using Image Inpainting", International Journal of Futuristic Science Engineering and Technology, vol. 1 Issue 2, ISSN 2320 – 4486, 2013

INNO SPACE
SJIF Scientific Journal Impact Factor

Impact Factor: 8.423

doi cross ref

ISSN INTERNATIONAL STANDARD SERIAL NUMBER INDIA

निस्केयर NISCAIR

INTERNATIONAL JOURNAL OF INNOVATIVE RESEARCH

IN SCIENCE | ENGINEERING | TECHNOLOGY

9940 572 462 6381 907 438 ijirset@gmail.com

www.ijirset.com

Scan to save the contact details